

Ongoing Efforts to Detect 21 cm Fluctuations of the Cosmic Dawn at the Owens Valley Long Wavelength Array (OVRO LWA)

Michael Eastwood, Gregg Hallinan, and Stephen Bourke
on behalf of the OVRO LWA and LEDA collaboration

mwestwood@astro.caltech.edu taucei.caltech.edu/mwestwood



The OVRO LWA

The Owens Valley Long Wavelength Array is a 288-antenna interferometer located at the Owens Valley Radio Observatory (OVRO) near Big Pine, California. Each antenna stand hosts a sky-noise-dominated, dual-polarization, broad-band dipole that covers 30 to 80 MHz. The OVRO LWA hosts the Large Aperture Experiment to Detect the Dark Ages (LEDA), which provides a back end that correlates 512 input signal paths with >50 MHz bandwidth and over 2000 frequency channels. 251 of the antennas are distributed within a compact 200 m diameter core, 32 antennas are placed out to ~2 km baselines, and the remaining 5 antennas are used by LEDA. In this poster I present the ongoing efforts to detect the spatial fluctuations of the 21 cm brightness temperature at redshifts $z > 20$. These measurements have the potential to revolutionize our understanding of star and galaxy formation.

The Cosmic Dawn

The term "cosmic dawn" refers to the epoch of early star formation prior to the epoch of reionization. Figure 3, shows how the amplitude of 21 cm brightness temperature fluctuations is expected to evolve with cosmic redshift. There is a peak near $z \sim 10$ corresponding to the epoch of reionization where the power spectrum is dominated by large ionized bubbles in the IGM. The power spectrum of these fluctuations at $z \sim 10$ is therefore sensitive to the properties of the ionizing sources. However, there is also a peak near $z \sim 20$ corresponding to the cosmic dawn.

At $z \sim 20$ early star formation produces X-ray sources that inhomogeneously heat the IGM, producing spatial fluctuations that may be measured with an interferometer (Pritchard & Furlanetto 2007). The supersonic motion of baryons relative to the dark matter following recombination suppresses star formation, generates enhanced 10 mK fluctuations, and imprints the signature of BAO oscillations into the spatial power spectrum (Tselikhovich & Hirata 2010). The timing and strength of Lyman-Werner feedback also plays a role (Visbal et al. 2012). A measurement of the spatial power spectrum of 21 cm emission at $z \sim 20$ will therefore be a window into the early universe and its star formation history that is distinct from the information learned at lower redshifts.

The field of view, collecting area, and compactness of the OVRO LWA suggests that this instrument will be a sensitive probe of HI at $z \sim 20$. However the path forward requires careful calibration, foreground mitigation, and characterization of the instrument.

Calibration

The OVRO LWA is made unique by its 30,000 baselines, entire-sky field-of-view, compactness, and 30 to 80 MHz frequency coverage. Traditionally an interferometer is calibrated by slewing to a known point source and solving for a modest number of complex gains. The OVRO LWA dipoles cannot slew, cannot put just a single point source in their beam, and the sky is not very well constrained in their frequency band. Furthermore, at such low frequencies refraction, scattering, attenuation, and Faraday rotation through the ionosphere become important.

In this regime it is necessary to have a fast and simple calibration routine that will allow rapid implementation of experimental calibration techniques. This is the motivation for TTCal, where the inner calibration loop is a mere 15 lines of code. TTCal is based on the work of Mitchell et al. 2008 and is freely available under an open source license (GPLv3+). Figures 4 and 5 were both generated using data calibrated by TTCal.

TTCal can solve for complex gains, Jones matrices, or gain amplitudes in a direction independent or direction dependent manner. Figure 4 shows a dirty image produced after Cas A and Cyg A have been calibrated and removed from the data set (they are restored after imaging). Figure 5 shows an all-sky image produced using m-mode analysis that may be used as a sky model to further improve the calibration.

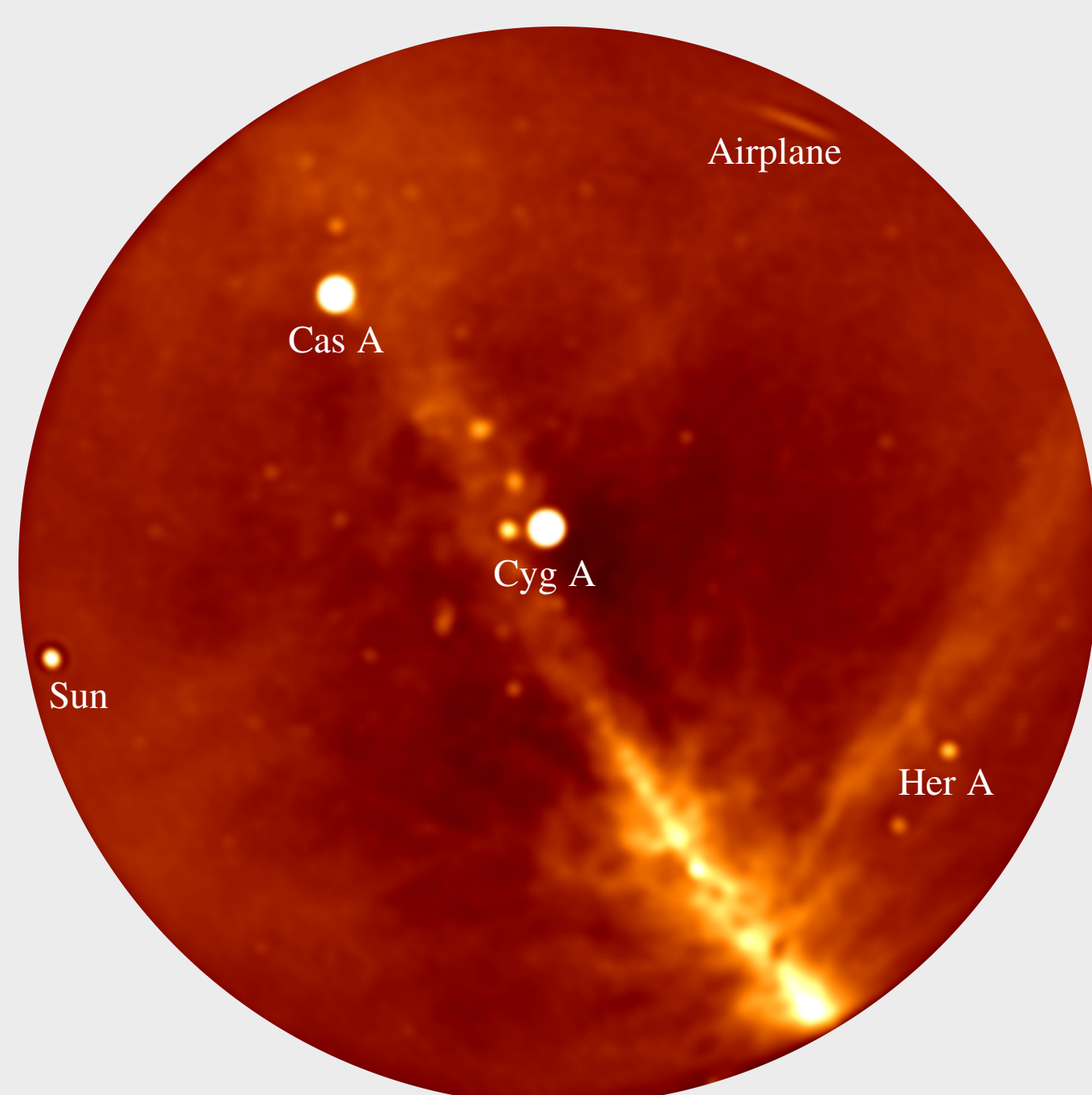


Figure 4. A dirty snapshot image of the sky as seen by the OVRO LWA (38 to 77 MHz). This image was made with a single 30 second integration using only the core antennas. Cas A and Cyg A were peeled from the data set using TTCal and restored to the image.

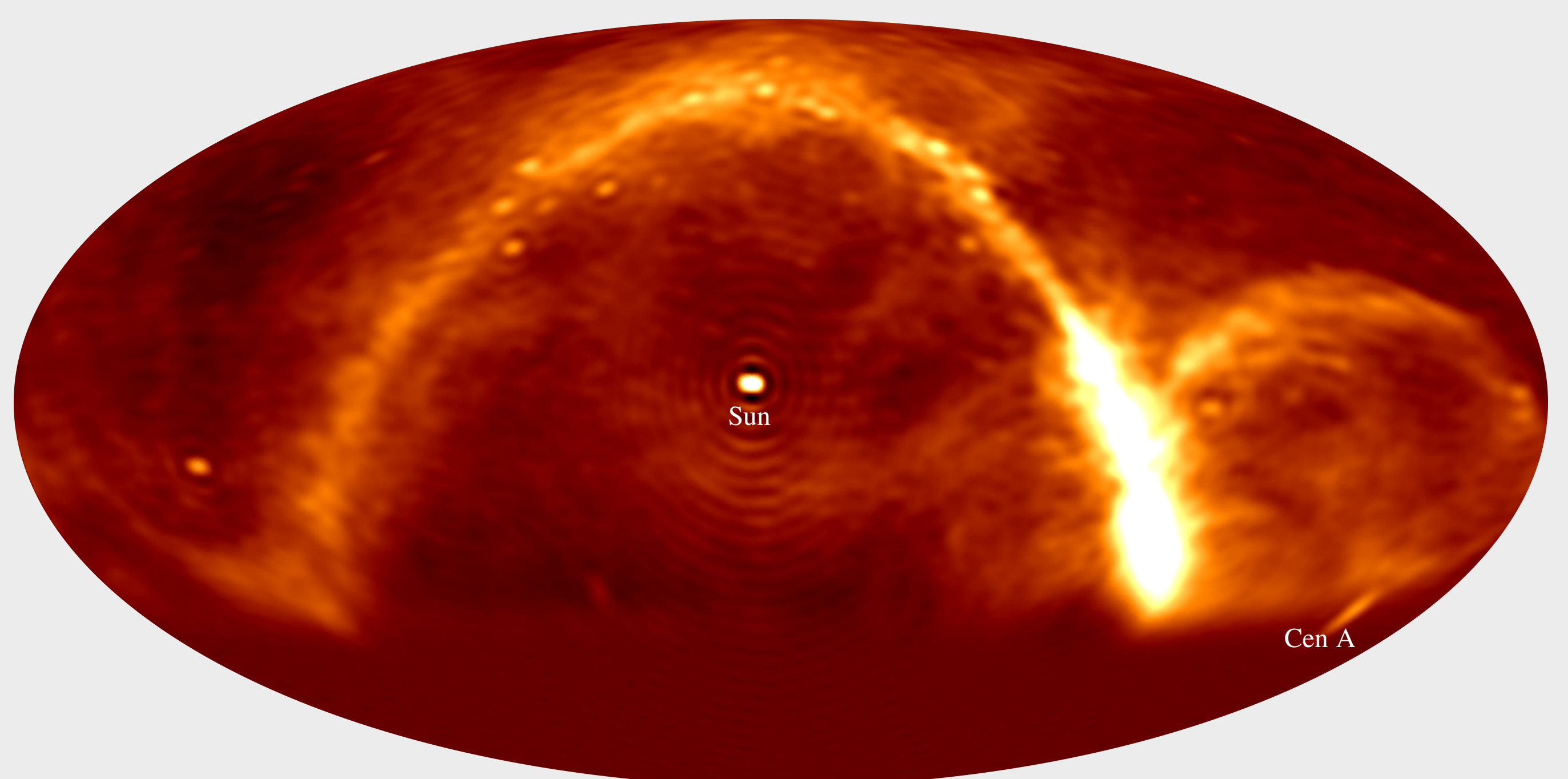


Figure 5. An all-sky image created by solving for the spherical harmonic coefficients using m-mode analysis. Several bright point sources (including Cas A and Cyg A) were crudely removed from the data set prior to imaging. This image uses 24 kHz bandwidth at 45 MHz, and was created from 288 thirty second integrations spanning a 24 hour period. This image was therefore created using 1/24000 of the data recorded in a 24 hr period. Note that the Sun is smeared slightly due to its motion through the sky.

Foreground Mitigation

The most commonly employed strategies for foreground mitigation can be broadly classified into two categories: foreground removal and foreground avoidance. In the former strategy, one attempts to model and subtract as much foreground emission as possible while leaving the 21 cm emission untouched. The latter strategy takes advantage of the fact that when attempting to measure a spatial power spectrum with a perfectly calibrated interferometer, spectrally smooth foreground emission can only corrupt a subset of the modes measured by the interferometer (ie. the "foreground wedge"). Therefore one can choose to measure modes that are not corrupted by the foreground emission (Parsons et al. 2012).

Each of these approaches has weaknesses. Foreground removal is an excellent choice for removing point sources, but subtracting diffuse emission is a much more complicated problem. Furthermore any subtraction strategy must make a decision about how to avoid removing the signal you are trying to measure. On the other hand, while foreground avoidance has proven that it can achieve sensitive upper limits on the 21 cm power spectrum (Ali et al. 2015), it struggles to suppress emission that leaks into the theoretically foreground-clean window (due to spectral unsmoothness in the instrument or the emission itself). Additionally the foreground contaminated modes contain a large fraction of the signal.

m-Mode Analysis

For a transit telescope such as the OVRO LWA, the respective limitations of foreground avoidance and removal can be avoided by the application of m-mode analysis (Shaw et al. 2014, Shaw et al. 2015). m-modes are the Fourier transform of a measured antenna correlation with respect to sidereal time (also referred to as a "fringe rate"). However, rewriting the visibility measurement equation in terms of m-modes simplifies to a matrix multiplication between a block-diagonal transfer matrix (which encodes the instrumental response) and the spherical harmonic coefficients of the sky.

$$\begin{pmatrix} \vdots \\ m\text{-modes} \\ \vdots \end{pmatrix} = \begin{pmatrix} \ddots & & \\ & \text{transfer matrix} & \\ & & \ddots \end{pmatrix} \begin{pmatrix} \vdots \\ a_{lm} \\ \vdots \end{pmatrix} \quad (1)$$

The block-diagonal nature of this equation means that only one value of m need be considered at a time. This is a major computational simplification. Furthermore a matrix equation is readily manipulated by all the standard tools of matrix analysis. For example, Equation 1 can be inverted (after conditioning) to solve for the spherical harmonic coefficients of the sky (see Figure 5).

Assuming the signal and foregrounds can both be modeled as Gaussian random fields (an assumption that is dubious for the galactic emission, but appears to work in practice), a Karhunen-Loeve transform can be used to construct a filter that retains all of the linear combinations of m-modes that are dominated by the expected cosmological signal. Quadratic estimators can then be used to calculate the power spectrum (Tegmark 1997).

Current Status

Ten days of data using just the core antennas has been collected and is being analyzed. An additional three days of data using the 32 recently installed long-baseline antennas has also been collected. The author is currently calculating the sensitivity of the OVRO LWA using the formalism of m-mode analysis and a realistic model of the interferometer. 2016 will see refined calibration and data analysis and additional data collection as data is accumulated in parallel with the OVRO LWA All-Sky Transient Monitor.



Figure 1. A map of California showing the location of the OVRO LWA.



Figure 2. A picture of an LWA antenna.

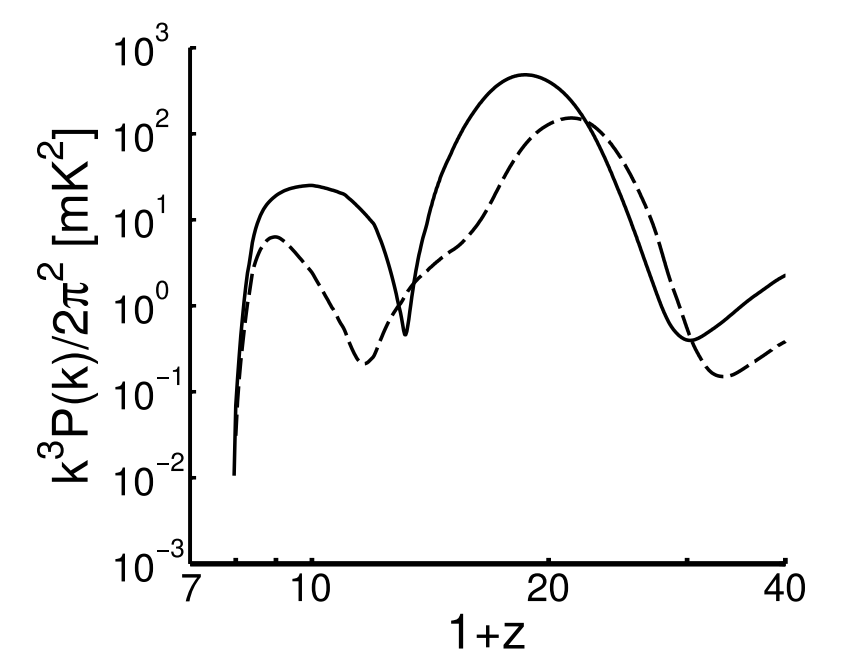


Figure 3. The evolution of a theoretical 21 cm spatial power spectrum (Fialkov & Barkana 2014). The solid line corresponds to $k = 1.0 \text{ Mpc}^{-1}$ and the dashed line corresponds to $k = 0.1 \text{ Mpc}^{-1}$.



TTCal

A calibration routine developed for the OVRO LWA. Freely available under an open source license (GPLv3+).
github.com/mwestwood/TTCal.jl